Review article

Jong-In Shim and Dong-Soo Shin*

Measuring the internal quantum efficiency of light-emitting diodes: towards accurate and reliable room-temperature characterization

Abstract: For accurate and reliable measurement of the internal quantum efficiency (IQE) of light-emitting diodes (LEDs), the method should be theoretically solid and experimentally simple to use without any prior assumption of physical parameters or complicated equipment. In this paper, we critically review the conventional characterization techniques for measuring the IQE of LEDs, including the methods based on temperature-dependent electroluminescence and constant AB(C) models. After reviewing the limitations of the existing IQE measurement techniques, we present the recently proposed method based on the improved AB model, called room-temperature reference-point method (RTRM). The RTRM is then applied to various LED devices to show how the IQE measurement techniques can be utilized to analyze their optoelectronic performances quantitatively.

Keywords: light-emitting diodes; internal quantum efficiency; characterization.

1 Introduction

Nowadays, light-emitting diodes (LEDs) are found in numerous applications for their many advantages such as low power consumption, small size, long lifetime, and fast switching. LEDs are available in various spectral ranges including ultraviolet, visible, and infrared wavelengths, based on different material systems [1–3]. Wide-bandgap materials such as GaN and associated alloys have been actively studied recently to achieve blue and UV emissions. While the LEDs are composed of simple pn junctions, there can exist multiple issues related with device configurations and materials. In order to analyze any possible device issues, accurate characterization of the device performance is an absolute necessity.

Many parameters have been utilized for LED devices to quantify the device performance so far: parameters obtained from simple current-voltage (*I-V*) and light-current (*L-I*) measurements constitute a basis, but they do not typically give enough details about a device under study [4–11]. Since many device parameters are interrelated, more extensive characterization is required to form a complete picture of the possible cause of the problem in the device and remedy it [12, 13]. At the same time, if there is any measure introduced to remedy and enhance the device performance, it is sometimes very difficult to judge whether the intended effects are achieved by simply checking the output parameters such as *I-V* and *L-I*.

Of the various device parameters, efficiencies contain the most important information on the device performance and any possible problem. Typically, the overall efficiency of the LED device is characterized by the power efficiency (PE), η_{PE}, defined by the ratio of the radiant power (optical power) from the LED to the input electrical power. The PE is rather simple to measure and serves as a useful parameter representing how efficient the device is in converting the electrical power to the desired radiant power; however, one needs to know more details than the PE to infer limiting factors in device performance.

The PE can be decomposed into its constituent factors, which are the voltage efficiency (VE), η_{VE}, and the external quantum efficiency (EQE), η_{EQE}. The EQE is then

*Corresponding author: Dong-Soo Shin, Department of Photonics and Nanoelectronics, Hanyang University ERICA, Ansan, Gyeonggi-do 15588, Republic of Korea; and Department of Bionanotechnology, Hanyang University ERICA, Ansan, Gyeonggi-do 15588, Republic of Korea, e-mail: dshin@hanyang.ac.kr.
http://orcid.org/0000-0002-0863-9138
Jong-In Shim: Department of Photonics and Nanoelectronics, Hanyang University ERICA, Ansan, Gyeonggi-do 15588, Republic of Korea. https://orcid.org/0000-0002-1305-074X

decomposed into the light-extraction efficiency (LEE), η_{LEE}, and the internal quantum efficiency (IQE), η_{IQE}. The IQE is in turn separated into the injection efficiency (IE), η_{IE}, and the radiative efficiency (RE), η_{RE}. In formula, they are expressed as follows:

$$\begin{aligned}\eta_{\text{PE}} &= \eta_{\text{VE}} \cdot \eta_{\text{EQE}} \\ &= \eta_{\text{VE}} \cdot \eta_{\text{LEE}} \cdot \eta_{\text{IQE}} \\ &= \eta_{\text{VE}} \cdot \eta_{\text{LEE}} \cdot \eta_{\text{IE}} \cdot \eta_{\text{RE}}. \end{aligned} \tag{1}$$

One can also define the active efficiency (AE), η_{AE}, by multiplying the VE and the IQE, i.e. $\eta_{\text{AE}} = \eta_{\text{VE}} \cdot \eta_{\text{IQE}}$, to characterize the overall performance of the active layer. The definitions of the efficiencies mentioned above are summarized in Table 1. These efficiencies represent respective conversion processes in the LED [1–3].

The PE, VE, and EQE are measurable by using experimental data of current, voltage, radiant power, and spectra. On the other hand, measuring the IQE has been a constant challenge. Thus, measuring the IQE accurately and reliably is extremely useful not only to elucidate the operating mechanisms of an LED device but also to improve the device performance.

2 Requirements for accurate and reliable IQE measurement

The first attempt to identify the IQE of an LED device is to theoretically calculate the LEE and measure the EQE as a function of DC bias current. Then the IQE is obtained by dividing the measured EQE by the calculated LEE. However, the LEE is quite sensitive to the microscopic parameters such as the imaginary refractive index of each material, the layer structure, or the randomly textured surface [14–16]. Theoretical calculation of the LEE is limited to a specific case in practice. Thus, direct measurement of the LED IQE as a function of current is more practical and has been pursued actively since the advent of LEDs in 1960s.

The IQE of an LED is a key parameter that represents the quality of epitaxial layers and contains essential

Table 1: Definitions of various LED efficiencies.

Efficiency	Definition
PE	$\eta_{\text{PE}} \equiv \dfrac{\text{radiant power}}{\text{electrical power}} = \dfrac{\Phi_e}{V_F I_F}$
VE	$\eta_{\text{VE}} \equiv \dfrac{\text{mean photon energy}}{\text{electron potential energy}} = \dfrac{h\overline{\nu}}{qV_F},\ h\overline{\nu} \equiv \dfrac{\Phi_e}{\int_0^\infty \dfrac{\lambda}{hc}\dfrac{d\Phi_e(\lambda)}{d\lambda}d\lambda}$
EQE	$\eta_{\text{EQE}} \equiv \dfrac{\text{\# of photons emitted to free space per second}}{\text{\# of electrons injected into the LED per second}} = \dfrac{\Phi_e/h\overline{\nu}}{I_F/q}$
LEE	$\eta_{\text{LEE}} \equiv \dfrac{\text{\# of photons emitted to free space per second}}{\text{\# of photons emitted from the active region per second}} = \dfrac{\Phi_e/h\overline{\nu}}{\Phi_{e,\text{active}}/h\overline{\nu}}$
IQE	$\eta_{\text{IQE}} \equiv \dfrac{\text{\# of photons emitted from the active region per second}}{\text{\# of electrons injected into the LED per second}} = \dfrac{\Phi_{e,\text{active}}/h\overline{\nu}}{I_F/q}$
IE	$\eta_{\text{IE}} \equiv \dfrac{\text{\# of electrons injected into the active region per second}}{\text{\# of electrons injected into the LED per second}} = \dfrac{I_{F,\text{active}}/q}{I_F/q}$
RE	$\eta_{\text{RE}} \equiv \dfrac{\text{\# of photons emitted from the active region per second}}{\text{\# of electrons injected into the active region per second}} = \dfrac{\Phi_{e,\text{active}}/h\overline{\nu}}{I_{F,\text{active}}/q}$
AE	$\eta_{\text{AE}} \equiv \dfrac{\text{radiant power emitted from the active region}}{\text{electrical power}} = \dfrac{\Phi_{e,\text{active}}}{V_F I_F}.$

The PE is also known as the wall-plug efficiency; the VE is sometimes referred to as the electrical efficiency. Φ_e, Radiant power; V_F, forward voltage; I_F, forward current; q, elementary charge; h, Planck constant; ν, frequency; λ, wavelength; c, speed of light in vacuum; $d\Phi_e(\lambda)/d\lambda$, spectral distribution; $\Phi_{e,\text{active}}$, radiant power emitted from the active region; $I_{F,\text{active}}$, forward current injected into the active region.

information on operational mechanisms such as the electron-hole recombination rate, the defect density, and carrier transport. As seen in Table 1, the IQE, defined as the ratio of the number of internally emitted photons to the number of electrically injected electrons, is the product of the IE and the RE. The IQE varies with the operating conditions of forward injection current I and temperature T as expressed below:

$$\eta_{\mathrm{IQE}}(I,\,T) = \eta_{\mathrm{IE}}(I,\,T) \cdot \eta_{\mathrm{RE}}(I,\,T). \tag{2}$$

The IE is a measure of how many electrons recombine in the active region compared to the total electrons injected into an LED. It generally depends on the current level as well as the LED structure itself. The RE can be thought of as the ratio of the radiative recombination rate to the total recombination rate (i.e. the sum of the radiative and non-radiative recombination rates) in the active region. For an accurate estimation of the IQE, it is necessary to consider the IE and the RE separately and quantitatively.

The IQE measurement methods satisfying the following requirements are desirable in view of accuracy, simplicity, reproducibility, and experimental system cost: (i) use only experimentally measurable physical quantities such as current and radiant power *without* assuming any physical parameters, e.g. chip sizes, epitaxial layer structures, carrier recombination rates, and complex refractive indices; (ii) measure the *relative* radiant power rather than the *absolute* radiant power for reducing measurement errors; and (iii) use measurement conditions of *operational* temperature and pumping scheme. The electroluminescence (EL) at room temperature is the most preferable combination compared with others. Finally, (iv) use CW pumping and its steady-state response of spontaneous emission, which eliminates the need for complicated and expensive experimental setups such as a short-pulse current driver, a high-speed photodetector, and an impedance matching technique for a good RF signal integrity.

In Section 3, we review the IQE measurement methods that have been popularly utilized so far, especially the methods based on temperature-dependent electroluminescence (TDEL) and constant AB(C) models. The technical problems involved in the conventional methods are deeply discussed. In order to overcome such limitations, a unique method of the IQE measurement, named as the room-temperature reference-point method (RTRM), has been proposed recently. The RTRM with its theoretical background is explained in Section 4. We then show an example of separately and quantitatively measuring LED efficiencies in Section 5 and finally conclude in Section 6.

3 Conventional IQE measurement methods: features and limitations

3.1 TDEL method

The TDEL method has been most popularly utilized with the longest history in the LED community and recognized as a standard method for IQE determination of LEDs [17–23]. This is partly due to the fact that it needs only a set of experimental data composed of the relative radiant power vs. forward current (Φ_e-I) at various temperatures including cryogenic temperatures. The disadvantage of the TDEL method is that it requires an expensive and very stable cryogenic system for long measurement time.

Two important assumptions are introduced in the TDEL method. The first is that the LEE is constant, independent of current and temperature, so that the EQE should be linearly proportional to the IQE for any I and T. This assumption enables finding the IQE at any I and T only by comparing the EQE in question with the EQE at a so-called reference current and temperature, I_{ref} and T_{ref}, at which the IQE is exactly known as $\eta_{\mathrm{IQE,\,ref}}$. In general, the reference point of I_{ref} and T_{ref} is selected for $\eta_{\mathrm{IQE,\,ref}} = 1$ such that both the IE and the RE must be 100% there. To find the reference point satisfying $\eta_{\mathrm{IE}} = \eta_{\mathrm{RE}} = 1$, the second assumption is used. At cryogenic temperatures, the nonradiative recombination centers in the active layer, which induce the Shockley-Read-Hall (SRH) recombination, are "frozen" and become inactive. Moreover, the direct Auger recombination rate in conventional semiconductors decreases exponentially with decreasing temperature so that the contribution of the Auger recombination rate is also neglected at the reference point. By assuming that both the SRH and Auger recombination rates are negligibly small at cryogenic temperatures, the RE is considered as 100% [24, 25]. In general, the assumption of $\eta_{\mathrm{RE}} = 1$ is experimentally confirmed by the fact that the peak EQEs at cryogenic temperatures do not increase further and maintain the maximum value with decreasing temperature.

With the RE of 100%, the EQE is linearly proportional to the IE so that the peak of the EQE should correspond to the maximum IE. In this method, the IE is also taken as 100% when it is experimentally confirmed that the peak value of the EQE does not vary with current in a limited range [19, 20]. As the reference point corresponding to an IQE of 100% is decided this way, the IQEs at other operating conditions are determined by taking the ratio as shown below:

$$\eta_{\text{IQE}}(I, T) = \frac{\eta_{\text{EQE}}(I, T)}{\eta_{\text{EQE}}(I_{\text{ref}}, T_{\text{ref}})}. \tag{3}$$

Note that η_{EQE} can be a relative EQE obtained from the relative radiant power since only the ratio is taken to obtain the IQE.

Next, we need to discuss a limitation in applying the TDEL method. Figure 1A and B shows different shapes of the relative EQE curves as a function of forward current at various temperatures for two blue LED samples. The samples are commercial LEDs from two different companies, both with lateral electrodes. The chip sizes and dominant wavelengths are $290 \times 590\ \mu m^2$ and 458 nm for the sample shown in Figure 1A and $280 \times 550\ \mu m^2$ and 447 nm for the one in Figure 1B. Figure 1A shows that the relative EQE maximum does not increase further at temperatures below 50 K. In this case, the IE and RE (thus IQE) can be assumed to be 100% and the IQE at operating conditions can be determined by Equation (3). However,

Figure 1: Two different relative EQE curves as a function of current at various temperatures: In (A), the EQE peaks saturate with decreasing temperature while in (B), they do not saturate.
It is thought that $\eta_{\text{IQE}} = \eta_{\text{IE}} = \eta_{\text{RE}} = 1$ in (A) while $\eta_{\text{IQE}} \neq 1$ ($\eta_{\text{IE}} \neq 1$) in (B) at their maximum EQE points.

some samples do not show such behaviors at cryogenic temperatures. In Figure 1B, the relative EQE maximums keep varying with decreasing temperature: the maximum of the relative EQE curves occurs at 100 K and then starts to decrease at temperatures lower than 100 K. In this case, the assumptions mentioned above are not satisfied: the TDEL method is *not* applicable to the LED samples showing this kind of behavior. The behavior is caused by the carrier leakage still remaining via processes like tunneling even with decreasing temperature, making the assumption that the maximum IE at the lowest cryogenic temperature is 100% invalid. This behavior is often observed with relatively highly defective samples. Thus, it is very important to note that the IQE determination by the TDEL method is not always possible: one must confirm whether the validity criterion with the relative EQE curves with temperature, as outlined above, is satisfied to apply the TDEL method to the LED sample under study.

Although the TDEL is a generally accepted method of measuring the IQE as a function of current only from the experimental EQE curves obtained at different temperatures ranging from room to cryogenic, it is very time- and labor-consuming. Lowering the temperature to cryogenic as low as ~20 K takes several hours using a helium closed-cycle system. Including preparation and actual measurements, the total testing would take a few hours. Thus, the needs for methods that can measure the IQE just at room temperature arise.
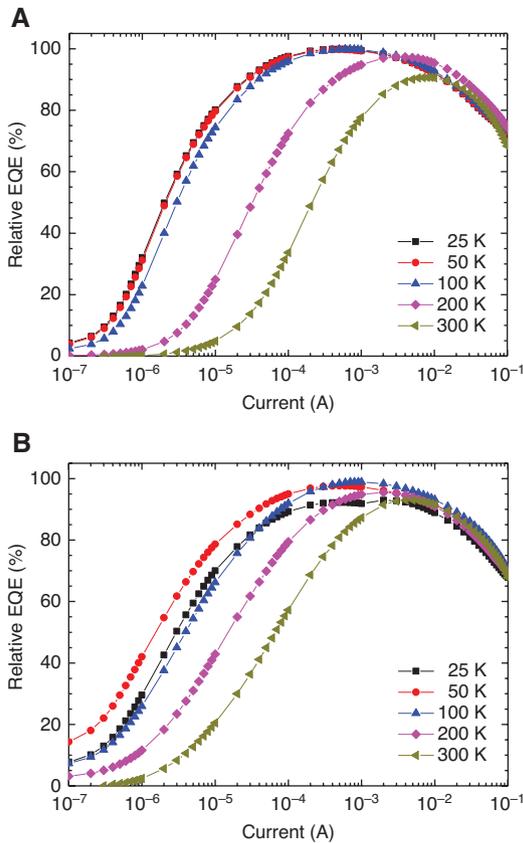
3.2 Constant ABC model

The simplest and the most popular method of the IQE measurement satisfying all the conditions of (i)–(iv) mentioned in Section 2 is the constant ABC model [26–42]. The model is based on the carrier rate equation for the LED (thus the name "ABC model"). Assumptions behind the model are as follows: (a) All carriers are injected into the active layers and recombine there. Thus, the IE is implicitly assumed as 100% with a well-defined active volume V_a. In this case, the IQE becomes identical to the RE. (b) Nonequilibrium concentrations of electrons and holes in the active layers are nearly equal to each other. (c) Three recombination processes, i.e. the nonradiative SRH, radiative band-to-band, and nonradiative Auger recombinations, are considered and their recombination rates are expressed with the recombination coefficients A, B, and C, respectively, and carrier concentration N. Note that A, B, and C coefficients are considered as certain *constants*. (d) Again, the LEE is independent of the injection current. Thus, the IQE has the same shape as the EQE as a function of current.

In the constant ABC model, a few noticeable results have been theoretically derived. First, the IQE or the EQE dependence on the injection current I is analytically expressed with two fitting parameters, the maximum IQE value, η_{max}, and the current, I_{max}, corresponding to η_{max} as follows [42]:

$$\overline{\eta}_{EQE} = \frac{1}{\eta_{max}} - \frac{(1-\eta_{max})}{2\eta_{max}}\left(1+\overline{\eta}_{EQE}\frac{I}{I_{max}}\right)\sqrt{\overline{\eta}_{EQE}\frac{I_{max}}{I}}, \quad (4)$$

where $\overline{\eta}_{EQE} = (\Phi_e/I)/(\Phi_{e,\,max}/I_{max})$ and Φ_e and $\Phi_{e,\,max}$ are radiant powers measured at currents I and I_{max}, respectively. Note that Equation (4) has no explicit dependence on the A, B, and C coefficients and is unambiguously determined only by I_{max} and η_{max} values where η_{max} and I_{max} satisfy the condition of $d\eta_{IQE}/dI = 0$. Since I_{max} is easily found experimentally by using the EQE vs. current relation, η_{max} is the only fitting parameter in Equation (4) in practice.

Second, A, B, and C coefficients are related to each other by η_{max} and I_{max} as

$$B = \frac{4\eta_{max}k}{I_{max}(1-\eta_{max})^2}A^2 \text{ and } C = \frac{4k^2}{I_{max}^2(1-\eta_{max})^2}A^3, \quad (5)$$

where $k = qV_a/\eta_{IE}$. Therefore, if one of the A, B, and C coefficients is known, the remaining coefficients can be obtained by using Equation (5) with the known quantities of η_{max}, I_{max}, and k. This is quite an unexpected result because A, B, and C constants represent different recombination processes, independent of each other.

The next task is to determine the maximum IQE value, η_{max} in Equation (4). Here, we introduce two approaches. The first is to select η_{max} that gives the best fit between the normalized experimental EQE and the simulated curves by Equation (4). The second approach of finding η_{max} is similar to the first: Equation (4) is rewritten as

$$\frac{1}{\overline{\eta}_{EQE}} = \eta_{max} + \frac{\overline{\Phi}_e^{1/2} + \overline{\Phi}_e^{-1/2}}{Q+2}, \eta_{max} = \frac{Q}{Q+2}, \quad (6)$$

where $\overline{\Phi}_e = \Phi_e/\Phi_{e,\,max}$ is the radiant power normalized by the peak EQE value. The factor $Q = B/\sqrt{AC}$ is a dimensionless invariant parameter and simply called Q factor. $\overline{\eta}_{EQE}$ and $\overline{\Phi}_e$ are experimental values of the EQE and the radiant power normalized by respective peak values. Plotting $1/\overline{\eta}_{EQE}$ vs. $\overline{\Phi}_e^{1/2} + \overline{\Phi}_e^{-1/2}$, approximating the plot by a linear function, and finding the intercept point of the line with the vertical axis, one can obtain the maximum IQE, η_{max}, and subsequently the Q factor [28, 37, 38].

The accuracy of the constant ABC model largely depends on finding an exact value of η_{max} so that a best fitting is usually taken around the EQE peak or I_{max}. However, one can often see that the data deviations from the ABC model predictions occur either at lower or higher currents from I_{max}. The mechanisms tentatively responsible for low- and high-current deviations from the ABC model predictions are introduced in detail in Refs. [35–42].

Apart from experimental discrepancies, the ABC model has a few theoretical limitations to be a reliable IQE measurement method. It should be remembered that this analysis is extremely dependent on many assumptions that are unverified in real-world devices. Some neglected complications can significantly alter the shape of the EQE curve and, thus, the parameter determination. The most suspicious assumptions are the following: (a) A, B, and C coefficients are not really constants but dependent on carrier concentration N and (b) the IE is not 100% but a function of current. Consequently, it is necessary to overcome theoretically and experimentally these technical hurdles arising from the constant ABC model for consistent and reliable measurement of the IQE values as a function of current.

3.3 Constant AB model

Two types of carrier losses related to the IE have been known: (i) nonradiative recombination through defects in the active layers and at the boundaries of the active layers (interfaces and surfaces) and (ii) leakage out of the active layers, i.e. carrier overflow. Usually, the two losses become important at low current levels far below the EQE peak and at high current levels beyond the EQE peak, respectively. In order to estimate the IQE exactly, each carrier loss needs to be identified quantitatively or at least relatively. However, the disentanglement of carrier losses into these two types is usually very difficult [42–45].

The restriction of the universal usage of the constant ABC model comes from the fact that the dominant nonradiative recombination process considered in the model at high current levels includes only the Auger recombination without identifying the influence of carrier overflow, i.e. the IE of 100% is always assumed with a well-defined active volume [41, 42]. Unfortunately, a method of discriminating between the Auger recombination and the carrier overflow experimentally is still controversial [36, 37].

The constant AB model has been developed in order to eliminate such an unclear problem of the IE at

high current levels involved in the constant ABC model [43–48]. The constant AB model is applied at low current levels around the onset of spontaneous emission in which the carrier loss of type (i) mentioned above becomes much more important than the carrier loss of type (ii). The crucial point is that all the losses of type (i) are thought to be directly proportional to the carrier concentration N in this regime. This means that all these losses can be lumped together in a single overall proportionality constant, or in a single effective nonradiative carrier lifetime τ_{nr}, which is independent of N. A simple theory shows that this approximation is reasonable when all the carrier recombination losses of type (i) have constant "saturated" recombination rates with a well-defined active volume. In this AB model, only an effective nonradiative recombination with a constant recombination coefficient A and the radiative recombination with another constant coefficient B are accounted for, under the assumption of an IE of 100% at low currents.

The fitting procedure from the experimental EQE curve as a function of current has been reported originally in Ref. [43] and recently in Ref. [47]. In this scheme, the IQE of an LED can be estimated from

$$\eta_{IQE} = \frac{\Phi_{e,12}^{1/2}}{\Phi_{0.5}^{1/2} + \Phi_{e,12}^{1/2}}, \tag{7}$$

where

$$\sqrt{\Phi_{0.5}} = \frac{\eta_{EQE,2} - \eta_{EQE,1}}{\eta_{EQE,1}/\sqrt{\Phi_{e,1}} - \eta_{EQE,2}/\sqrt{\Phi_{e,2}}} \text{ and } \Phi_{e,12} = \frac{\Phi_{e,1} + \Phi_{e,2}}{2}. \tag{8}$$

In Equations (7) and (8), $\Phi_e = \eta_{LEE} h\bar{v} V_a B N^2$ is the radiant power of the LED with the active volume V_a and nonequilibrium electron/hole concentration N. $\Phi_{0.5} = \eta_{LEE} h\bar{v} V_a A^2 B^{-1}$ is the radiant power corresponding to an IQE of 50%. $\eta_{EQE,j}$ and $\Phi_{e,j}$, where $j = 1, 2$, are the EQE and the radiant power of the LED measured at two different driving currents. Just for an IQE, it is not necessary for $\eta_{EQE,j}$ to be an absolute value. However, if the LEE is to be found, the absolute EQE value is required.

The constant AB model works well in some advanced LEDs where all the carrier losses of type (i) are so small that they are easily saturated at very small currents [46]. In reality, however, there are still many LED chips that have large and unsaturated carrier losses of type (i). Therefore, it is necessary to check the assumptions of an IE of 100% and the constancy of A and B recombination coefficients before applying the constant AB model [48–50].

4 The RTRM

4.1 Theoretical background of the RTRM

The RTRM is a method to solve the technical problems in the constant ABC and AB models [51]. This improved model includes the following elements: (a) the recombination coefficients of A, B, and C are not constant but depends on the carrier concentration N; (b) the nonradiative Auger recombination is negligibly small at low currents below from the maximum EQE current, I_{max}. In this current range, the AB model instead of the ABC model is possible; (c) the IE is a function of current I or carrier concentration N so that there is a certain current, called the reference current I_{ref}, where the IE is maximized; and (d) the LEE is assumed as constant so that the shape of an experimentally observed EQE curve is the same as that of the IQE curve. Thus, the IQE dependence on current can be obtained once an IQE is exactly known at one point of the reference current I_{ref}. This approach is very similar to the TDEL where operating conditions of the current and cryogenic temperature are searched for the IQE to be assumed as 100%; and (e) the IE at I_{ref} is considered as high as 100% if any special attention is not required.

In the AB model, the spontaneous radiant power detected by a photodetector Φ_e and the injection current I can be epxresssed by a simple quadratic equation as shown below:

$$Y = a_1 X + a_2 X^2, \tag{9}$$

where $Y = I/I_p$, $X = \sqrt{\Phi_e(I)/\Phi_e(I_{max})}$. The a_1 and a_2 coefficients are dependent on current I and are given by

$$a_1(I) = K_1 \frac{1}{\sqrt{B(I)}} \frac{A(I)}{\eta_{IE}(I)} \text{ and } a_2(I) = K_2 \frac{1}{\eta_{IE}(I)}, \tag{10}$$

where K_1 and K_2 are constants. All other parameters of X, Y, a_1, a_2, A, B, and η_{IE} are functions of current I. Note that both X and Y are experimentally obtained parameters.

Here, we consider two paths of carrier losses recombining outside the active layers: (i) defect-related leakage current I_{defect} via surface, hetero-interface, or other defective areas and (ii) overflow leakage current $I_{overflow}$ surpassing the active layers. These leakage currents result in the IE not being ideal. As the forward voltage increases, the defect-related leakage current I_{defect} appears at low bias voltages and saturates at a finite density of trapping centers. Then, most of the carriers begin to inject into the active layers and recombine there with the IE increasing. As the bias voltage increases further, $I_{overflow}$ starts to flow

at a certain bias and becomes a dominant leakage-current component over I_{defect}, which in turn decreases the IE again. In this picture, there will be a certain current, called the reference current I_{ref}, at which the IE is maximized.

Our idea to find I_{ref} is as follows: As the current I increases, a_1 and a_2 generally vary very slowly compared to X and Y. Thus, the functions a_1 and a_2 are obtained by solving two simultaneous equations of (9) with two nearest experimental data (X_i, Y_i) and (X_{i+1}, Y_{i+1}). In Equation (10), the a_2 coefficient is inversely proportional only to the IE. Thus, we select I_{ref} as a current at which a_2 is the minimum.

As a first step, we assume $\eta_{IE} = 1$ at $I = I_{ref}$ in that I_{defect} saturates at a much smaller current than I_{ref}, i.e. $I_{defect} << I_{ref}$ and $I_{overflow}$ is not so large yet. The IQE estimation errors due to this assumption is discussed in the next section. $\eta_{RE}(I_{ref})$ is then found for the set of $(X_{ref}, a_{1, ref}, a_{2, ref})$ at I_{ref}, using $\eta_{RE} = a_2 X^2 / (a_1 X + a_2 X^2)$. Subsequently, η_{IQE} at I_{ref}, i.e. $\eta_{IQE}(I_{ref})$, is obtained by using already known values of $\eta_{IE} = 1$ at I_{ref}.

Finally, we can calculate $\eta_{IQE}(I)$ at any current I with a known value of $\eta_{IQE}(I_{ref})$ from

$$\eta_{IQE}(I) = \eta_{IQE}(I_{ref}) \frac{\eta_{EQE}(I)}{\eta_{EQE}(I_{ref})}. \tag{11}$$

Table 2 summarizes the IQE measurement methods discussed so far.

4.2 The RTRM vs. TDEL and constant ABC model: comparison

We apply three IQE measurement methods of the TDEL, the constant ABC model, and the RTRM to a same blue LED chip and compare the results. A commercial lateral-type InGaN/GaN multiple-quantum-well blue LED grown on a c-plane sapphire substrate with a chip size of $1100 \times 650 \ \mu m^2$ has been selected.

The LED was driven under the pulsed-current driving condition (pulse period: 1 ms, duty cycle: 1%) for minimum self heating. The LED sample was cooled down from 300 to 20 K in a helium closed-cycle cryostat by Advanced Research System.

Radiant powers from the sample measured at various temperatures are shown in Figure 2. The maximum radiant power at 250 mA is obtained at a medium temperature of 200 K, not at the lowest cryogenic temperature of 20 K, which is due to efficiency droops acting differently with current and temperature. Shown in Figure 3A are emission

Table 2: Summary of IQE measurement methods utilizing the electrical pumping and DC response.

| Method	IQE measurement procedure	Notes
Calculation of LEE	– Calculate the LEE – Measure the absolute EQE – Calculate the IQE (=EQE/LEE)	– Structural and material parameters are assumed – Absolute EQE measurement at room temperature
TDEL	– Measure the relative EQE curves at various temperatures including cryogenic temperatures – Find a reference IQE at saturated peak EQEs – Calculate the IQE at room temperature	– Relative EQE measurements at various temperatures – $\eta_{IQE} = \eta_{IE} = \eta_{RE} = 1$ at saturated EQE peaks – Constant LEE over temperatures and currents
Constant ABC model	– Measure the relative EQE curve – Find a peak IQE or constant ABC coefficients by best fitting the EQE curve – Calculate the IQE	– Relative EQE measurement at room temperature – Constant A, B, C; $\eta_{IE} = 1$ – Constant LEE over currents
Constant AB model	– Measure the relative EQE curve – Find the LEE or AB coefficients by best fitting the EQE curve – Calculate the IQE	– Relative EQE measurement at room temperature – Constant A, B; $\eta_{IE} = 1$ – Constant LEE over currents
RTRM	– Measure the relative EQE curve at room temperature – Find the IQE just at a reference point – Calculate the IQE curve	– Relative EQE measurement at room temperature – $\eta_{IE} = 1$ just at a reference point – Constant LEE over currents
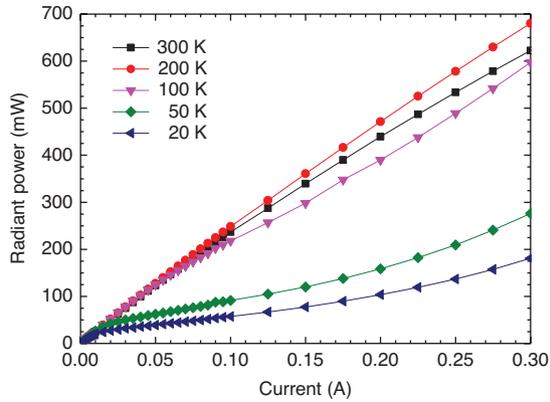
Figure 2: Radiant power vs. current of a blue LED sample measured at various temperatures.
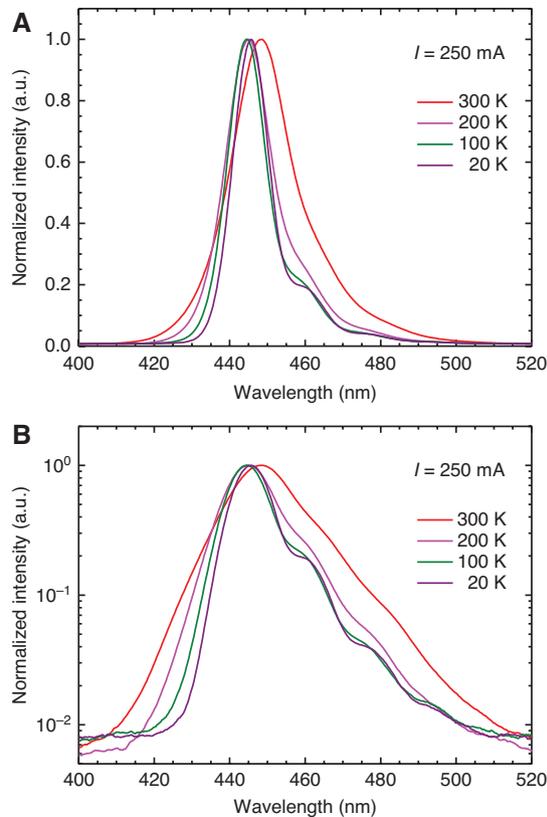

Figure 3: The peak wavelength shows the U-like shift as temperature decreases.
Normalized intensities on (A) linear and (B) log scales measured at various temperatures.

spectra on a linear scale at a current of 250 mA for various temperatures. As temperature decreases from 300 K to 200, 100, and 20 K, the peak wavelength shows the U-like shift from 448 nm to 445, 444, and 445 nm, respectively. We believe that this U-like shift of the peak wavelength is due to a tradeoff between the bandgap widening and the

thermal heating by increasing resistance. It is also seen that a subpeak around 460 nm becomes more pronounced. Actually, there are a series of subpeaks when the emission spectra are plotted on a log scale (Figure 3B). The more pronounced subpeaks with decreasing temperature have been reported as the longitudinal-optical (LO) phonon replicas of the main peak [52, 53]. On the other hand, an LED chip has finite reflectivities at the interfaces between metallic surfaces, epitaxial layers, and substrate surfaces. Since the optical losses are reduced with decreasing temperature, the Fabry-Perot effect is another possibility of the subpeaks. More investigation is necessary to further identify the exact cause of the subpeaks.

The *I-V* characteristics measured at various temperatures are depicted in Figure 4. It is seen in the reverse-bias region that the generation currents via defects at reverse biases less than −5 V are negligible at all temperatures and become smaller with decreasing temperature. On the other hand, it is not easy in the forward-bias region to identify the amount of leakage currents that do not recombine in the active layers. Here, we follow the RTRM in order to find the leakage current at relatively low current levels.

Figure 5 depicts a_2 obtained by solving two simultaneous equations for two nearest experimental data from the converted *X-Y* graph according to Equations (9) and (10). For this sample, the obtained a_2 is not constant, implying that $\eta_{IE} \neq 1$ over the current ranges investigated. At 300 K, a_2 decreases for currents beyond ~10^{-5} A, approaches a minimum at 2×10^{-3} A ($=I_{ref}$), and then increases. This indicates that the IE, inversely proportional to a_2, approaches a maximum, which is considered as 100%, and then decreases. For very small currents below ~10^{-5} A denoted as region I, the rapid change in a_2 could be due to the leakage current I_{defect} before the onset of the radiative current flowing into the active layers. It should be noted that such
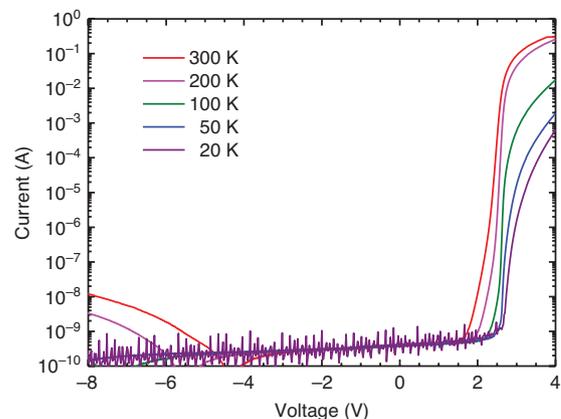

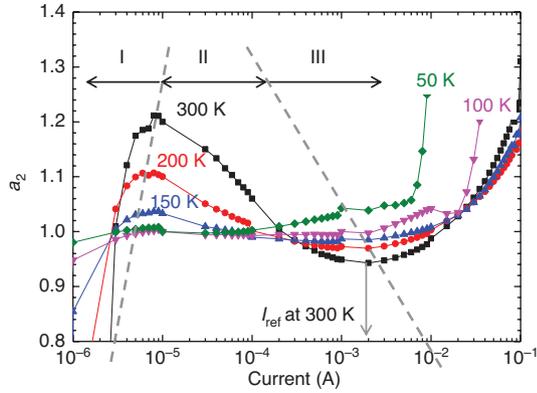**Figure 4:** *I-V* characteristics at various temperatures.

Figure 5: Calculated a_2 as a function of current for various temperatures.
I_{ref} at 300 K is the current giving the minimum value of a_2 in region II.

a leakage current is different in each device and operating condition so that we should pay attention to the influence of the leakage on the IQE calculation in every IQE measurement. For a current range of 10^{-5}–2×10^{-3} A, denoted as region II, a_2 decreases and the IE increases. This is due to the saturated I_{defect} and the monotonic increase of the radiative current. For $I > I_{ref}$ as denoted in region III, the carrier overflow from the InGaN quantum wells to the p-GaN clad layer should be responsible for the increasing a_2 and decreasing η_{IE}. As the temperature is decreased, it is seen that a_2 becomes flattened near the minimum, indicating that η_{IE} does not vary as much as at room temperature. This is reasonable because η_{IE} is not expected to change much at cryogenic temperatures with vanishing leakage paths owing to the defect freeze-out. This trend is confirmed later with the TDEL measurements (Figure 6).

Figure 6 shows the measured IQEs as functions of current by applying the TDEL (solid lines) and the RTRM (symbols). The IQEs at the reference currents from
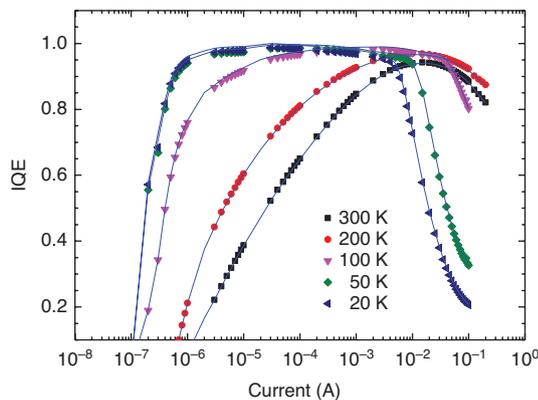
Equation (10) are estimated to be 0.876, 0.959, and 0.978 for 300, 150, and 20 K, respectively, and other IQE values are calculated by using Equation (11). The maximum EQE at the cryogenic temperature is selected as IQE of 100% ($I_{ref} = 2 \times 10^{-5}$ A, $T_{ref} = 20$ K in this case) and $\eta_{IQE}(I, T)$ at any temperature T is calculated from Equation (3). In TDEL, one should pay attention to experimentally confirming the saturation characteristics of the maximum η_{EQE} at the reference point by changing both temperature and current. As shown in Figure 6 by solid lines, $\eta_{IQE} > 99\%$ are measured at certain current ranges (7×10^{-6}–2×10^{-4} A for 20 K and 2×10^{-5}–5×10^{-4} A for 50 K).

The calculation procedures of the two methods, the RTRM and the TDEL, are very similar once η_{IQE} at a reference point is found. η_{IQE}'s at other currents are then calculated from η_{IQE} at the reference point by taking the relative ratios from the experimental η_{EQE} values. Thus, the shapes of the IQE curves at a certain temperature by the two methods are identical except the peak IQE values. The maximum η_{IQE}'s by the TDEL and RTRM at 300 K are almost the same as 0.941 and 0.943, respectively. The maximum IQEs by the two different methods agree very well within 2% for all temperatures. The small discrepancy in the maximum η_{IQE} obtained by the two methods could occur from the measurement inaccuracies in radiant power as well as the temperature dependency of the LEE [23]. The LEE can vary with temperature especially when the energy of the spontaneous emission from the active layer of an LED is close to the bandgap energy or absorption edge of the surrounding materials. Variations in LEE with InGaN-based LEDs have been reported to be as much as 4–6% over temperatures from ~10 to 300 K [23, 54, 55].

Finally, we discuss the error involved in the RTRM by assuming $\eta_{IE} = 1$ at I_{ref}. Using the data obtained at 300 K, the left axis of Figure 7 shows $a_2(I_{ref})/a_2(I)$, which

Figure 6: IQEs obtained by the RTRM (symbols) and TDEL (solid lines) at various temperatures.
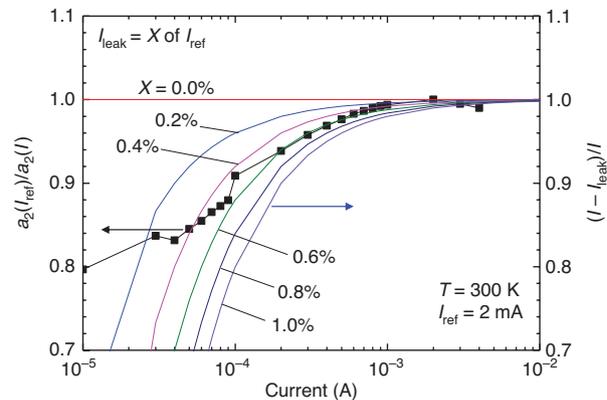

Figure 7: Comparison of the IE obtained from a_2 at 300 K (left axis) and the theoretical IE for constant I_{leak} (right axis).

represents the IE. On the right axis, the theoretical IE, that is, $(I - I_{leak})/I$, is given for a *constant* leakage current I_{leak}: naturally, the theoretical IE quickly approaches unity as the total current increases. From the various ratio of I_{leak} to I_{ref}, it is seen that the IE from a_2 roughly follows the functional shape of the theoretical IE between the leakage of 0.4% and 0.6% of I_{ref}. This indicates that at I_{ref}, the IE is considered to be 99.4% in the worst case. From this exercise, we think that the assumption of $\eta_{IE} = 1$ is reasonable, with only a minimal error included. Samples with very high leakage currents, however, should be treated carefully as they may not satisfy the assumption $\eta_{IE} = 1$ at I_{ref}.

In fact, theoretical background of the constant AB model is quite similar to that of the RTRM except that the former utilizes a wide range of relatively low current levels with $\eta_{IE} = 1$ and the latter selects one reference current with $\eta_{IE} = 1$. Thus, the key is to find the current at which the assumption of $\eta_{IE} = 1$. In this sense, we can get a lot of information from the calculation of a_2 as a function of current as demonstrated in Figure 5.

We also try to fit the experimental data measured at 300 K by using the constant ABC model [Equation (4)]. The sample under test has $I_{max} = 15$ mA so that we can theoretically calculate the normalized EQE curve with η_{max} as a fitting parameter and compare it with the one obtained from the experiment (Figure 8). It is seen that $\eta_{max} = 90\%$ gives the best fit for the data near I_{max}. Still, deviations from the experimental data are observed for lower and higher currents than I_{max}.

Using the η_{max} value obtained by this fitting, we plot the relative ratios of the SRH, radiative, and Auger recombination currents to the total current (Figure 9). At $I_{ref} = 2$ mA of the RTRM, denoted by the dotted line, it is seen that the Auger recombination current in the constant ABC model is 1.6% of the total current. With this level of contribution of the Auger recombination, we
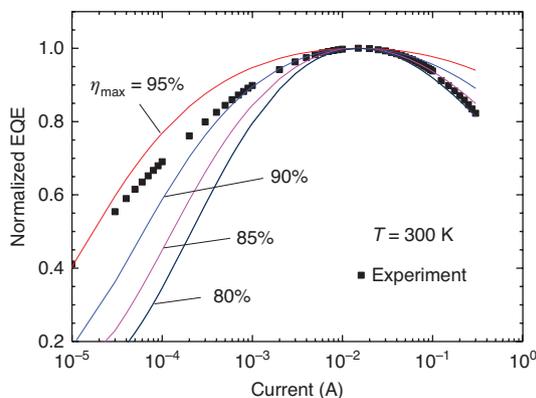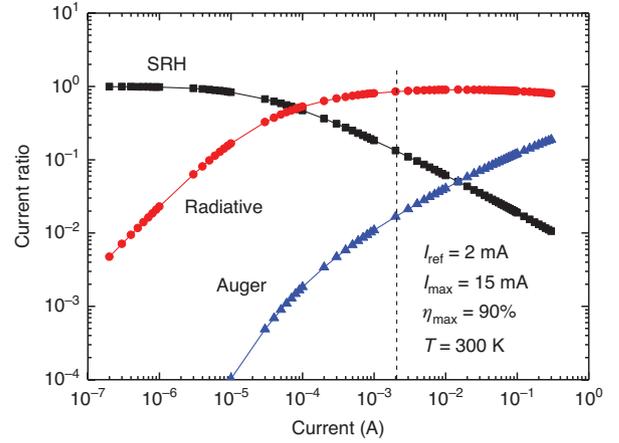

Figure 9: Ratio of the SRH, radiative, Auger recombination currents to the total current.

think that the Auger recombination term can be neglected for finding the reference point in the RTRM method. In fact, the Auger recombination current in the constant ABC model can correspond to the current leakage via carrier overflow in the RTRM for certain constant A and B coefficients. In this picture, this negligible Auger recombination current at I_{ref} can be considered as another vindication that the carrier leakage can be neglected at the reference point in the RTRM.

We have compared three IQE measurement methods of the RTRM, the TDEL, and the constant ABC model. All three methods have been developed to utilize the experimentally measured EQE curve. In the TDEL, the IQE of 100% at a cryogenic temperature is found by changing both temperature and current for a simultaneous condition satisfaction of $\eta_{IE} = \eta_{RE} = 1$. The IQE at room temperature is then calculated by the relative ratio of the EQE values at room temperature to the cryogenic reference point under the assumption of a constant LEE for all temperatures. In fact, the LEE of an LED may not be constant: it typically becomes smaller at higher temperature. Moreover, the temperature dependence of the EQE becomes larger as the emission wavelength of an LED becomes longer from visible to infrared spectral ranges. This results from the increase of optical losses in epitaxial layers whose bandgap energies are not so much different from that of the active layer. Therefore, the TDEL can be recommended to be used for InGaN-based visible LEDs rather than longer-wavelength GaAs- or InP-based LEDs. On the other hand, the RTRM and the constant AB(C) models under a given temperature assume only the constant LEE with current, which is more reasonable than in the TDEL.

Figure 8: Normalized IQEs by the RTRM and the constant ABC model.

The conventional constant AB(C) models roughly assume the IE of 100% for certain current ranges near the onset of light emission or the EQE peak. In real LEDs, however, it is hardly true that the IE is perfect since the leakage current via defects near the onset of light emission and the carrier overflow near the EQE peak are frequently observed. The RTRM overcomes such technical hurdles in the conventional AB(C) models. From this consideration, we think that the RTRM is the most accurate and reliable of all the methods considered herein.

5 Application of the RTRM

5.1 Various LED efficiency measurements

Here, we demonstrate how one can measure various LED efficiencies constituting the PE. As individual efficiencies represent different physical processes, separating various efficiencies is very beneficial in remedying any problems and enhancing the performance of LED chips further. For this purpose, we prepared a commercial lateral-type InGaN/GaN multiple-quantum-well blue LED grown on a c-plane sapphire substrate with a chip size of $740 \times 600~\mu m^2$. The peak wavelength is ~450 nm at 293 K. The LED was driven under the pulsed-current driving condition (pulse period: 1 ms, duty cycle: 1%) by a Keithley sourcemeter 2602B. The pulsed-current driving here is for avoiding the self-heating effect and is not essential for the IQE measurement by the RTRM: measurement of the radiant power by the CW current injection is also OK even though the chip is heated at high currents. The IQE measured under CW current injection may reflect the IQE in real operating conditions. If one wants to measure the intrinsic LED characteristics at a given chip temperature, however, the pulsed-current driving is recommended. The response of an LED operated under this pulsed-current injection is still considered as steady state since the pulse is relatively long (in the order of 1 ms).

In the following example, we measure the absolute radiant power, not the relative radiant power, since the PE, EQE, and LEE measurements require the absolute radiant power. If one wants to measure the IQE only, the measurement of the relative radiant power is sufficient.

Figure 10 is a flow chart of measuring various LED efficiencies separately and quantitatively. We follow each step and show how the measurement of each efficiency is possible.

First, the PE should be obtained from the radiant power (voltage) vs. current measurement (Figure 11). Once
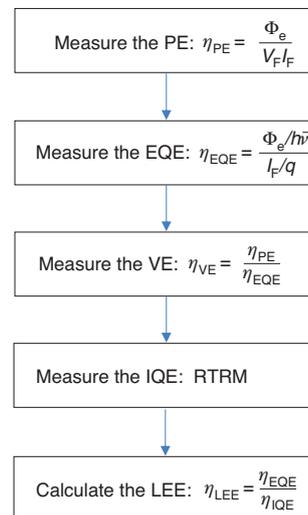

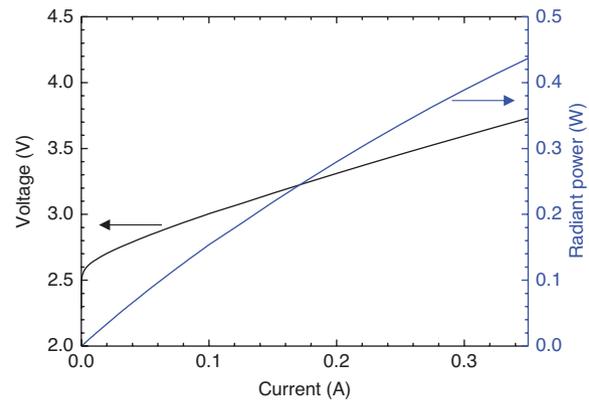**Figure 10:** Flow chart for the LED efficiency measurements.

Figure 11: Radiant power and forward voltage as a function of forward current.

the radiant power and forward voltage are obtained as a function of current, the PE can be evaluated by taking the ratio of the radiant power to the input electrical power, as depicted by line 1 in Figure 12.

Second, measure the emission spectra and calculate the mean photon energy as defined in Table 1. Figure 13A and B shows the emission spectra at various injection currents and the mean photon energy thus obtained. Using definitions given in Table 1, calculate the EQE by taking the ratio of the number of photons emitted to free space per second to the number of electrons injected into the LED per second. The result is shown as line 2 in Figure 12.

Third, now calculate the VE by taking the ratio of the PE to the EQE, whose result is shown as line 3 in Figure 12. Note that at currents below ~20 mA, the VE exceeds 100%, indicating that the mean photon energy is actually larger than the electron potential energy supplied by the source,
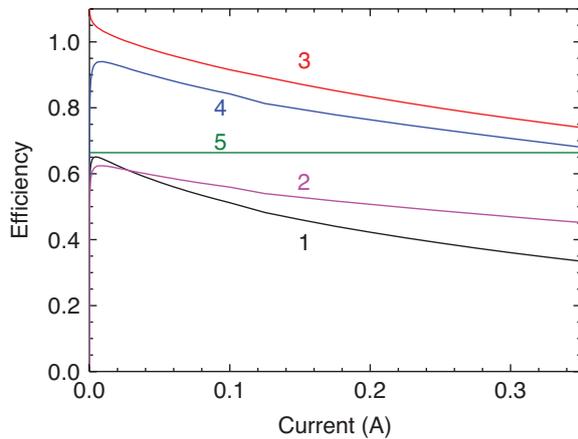
Figure 12: LED efficiencies as a function of forward current. 1: PE; 2: EQE; 3: VE; 4: IQE; 5: LEE.
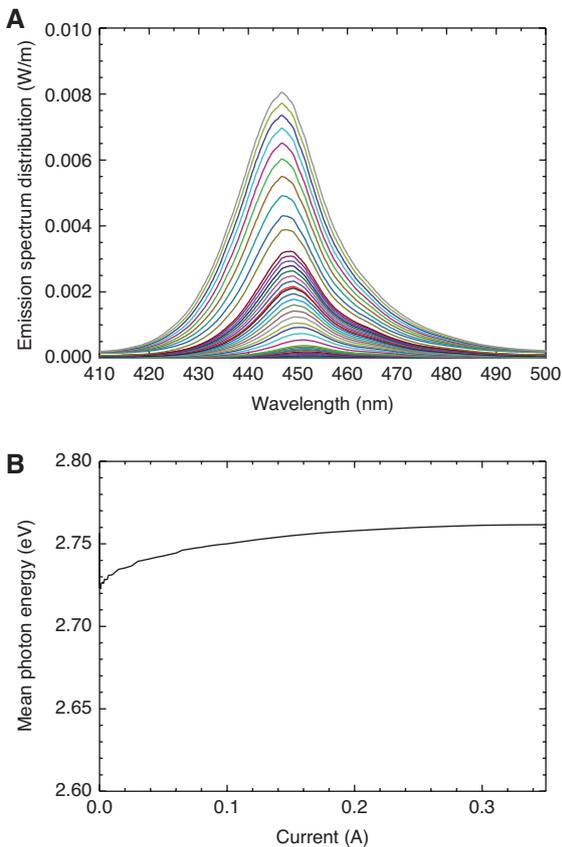

Figure 13: Below ~20 mA, the mean photon energy is larger than the electron potential energy supplied by the source. (A) Emission spectra in the current range of 1 μA to 350 mA and (B) the mean photon energy as a function of forward current.

the fact only possible when one includes thermal energy into account. At voltages lower than the mean photon energy divided by the elementary charge, the carriers are still injected into the active region with the help of thermal

energy in the lattice. This interesting phenomenon has been reported elsewhere by various names such as electroluminescent refrigeration, opto-thermistic cooling, or thermo-photonic cooling since the cooling of the lattice occurs when the carriers take away the thermal energy from the lattice and get injected into the junction [56–58].

Fourth, now one needs to measure the IQE accurately. Using the RTRM, the IQE is obtained as shown by line 4 in Figure 12.

Lastly, once the IQE is obtained, the LEE can be obtained by taking the ratio of the EQE to the IQE. The LEE thus obtained is ~66% (line 5 in Figure 12). The key LED efficiencies of PE, EQE, VE, IQE, and LEE have thus been measured separately and quantitatively, giving important information on the respective physical processes.

5.2 IQE vs. forward voltage

Although the performances of InGaN-based LEDs have significantly improved, a higher PE is still desired. Improving the PE requires enhancing the EQE and reducing the forward voltage simultaneously. While it has been recognized experimentally that both the EQE and the forward voltage are interactively dependent on epitaxial growth conditions in some cases, they have so far been studied independently as the so-called "efficiency droop" and the ohmic problem.

To have a higher EQE, one needs to optimize the epitaxial layer structure, especially the active layers. However, the variation in LEE can mask the actual changes in active layers and confuses the trends in EQE experiments. In order to avoid the confusion caused by the LEE variation and focus only on the active layer properties, one needs to use the IQE, not the EQE. At the same time, the changes in forward voltage with epitaxial-structure modification should also be tracked. With the reliable IQE measurement such as the RTRM, investigating the correlation between the IQE and the forward voltage has become possible.

We have tested 45 InGaN/GaN multiple-quantum-well blue LEDs with three different chip types, fabricated by a single company. The growth condition for the active epitaxial layers of each LED chip is slightly different. Figure 14 shows the relationship between the forward voltage and the IQE at a current density of 25 A/cm². Although these LEDs have been fabricated by identical processes, it is clear that there is an inverse relation between the IQE and the forward voltage for different sets of active-epitaxial-layer growth conditions. This is the first systematic experimental result that the forward voltage is not solely determined by ohmic resistance: the carrier
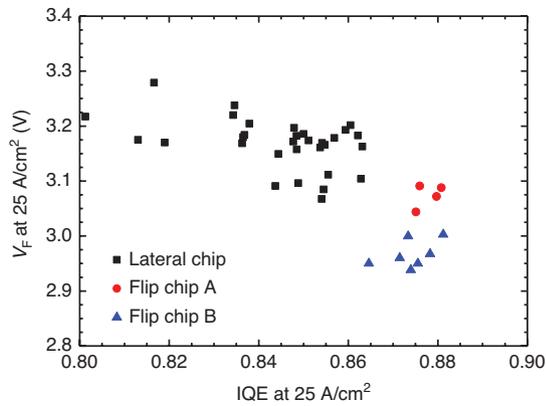
Figure 14: Forward voltage vs. IQE of various blue LEDs measured at 25 A/cm².
The chip sizes for different electrode types are $960 \times 620 \, \mu m^2$ (■), $1400 \times 1400 \, \mu m^2$ (●), and $850 \times 850 \, \mu m^2$ (▲).

recombination rate in the active region plays a key role in LED devices. More details on the physical origin behind this observation require further investigation.

6 Conclusion

Measuring the IQE has a key importance in characterizing the LED performance and finding the detailed information on the physical processes in the LED. While there have been conventional methods of measuring the LED IQE such as the TDEL and constant AB(C) models, they have clear limitations in applying the method for various LEDs owing to specific assumptions utilized to obtain the IQE values as reviewed in Section 3. For example, the method based on the constant ABC model cannot fit the experimental data away from the EQE peak, which is due to the very rough assumption that $\eta_{IE} = 1$ for all current ranges. The more advanced RTRM eliminates this assumption, thus making it possible to measure the IQE as a function of current accurately. Moreover, the RTRM can be applied easily and reliably since it requires only the relative EQE curve as a function of current just at room temperature.

We have applied the RTRM method to a blue LED and obtained various LED efficiencies of PE, VE, EQE, IQE, and LEE. It has also been revealed experimentally that the forward voltage of LEDs has a close relationship with the IQE, thus the carrier recombination rate in the active region. An accurate and reliable measuring method of the LED IQE such as the RTRM should greatly help elucidate the operational mechanisms of LEDs and improve the device performance further.

References

[1] Seong TY, Han J, Amano H, Morkoc H. III-Nitride based light emitting diodes and applications. Heidelberg, Springer, 2017.

[2] Khanna VK. Fundamentals of solid-state lighting. New York, CRC Press, 2014.

[3] Schubert EF. Light-emitting diodes. 2nd ed. Cambridge, Cambridge University Press, 2006.

[4] Lee SW, Oh DC, Goto H, et al. Origin of forward leakage current in GaN-based light-emitting devices. Appl Phys Lett 2006;89:132117.

[5] Mao A, Cho J, Dai Q. Characteristics of dotlike green satellite emission in GaInN light emitting diodes. Appl Phys Lett 2011;98:023503.

[6] Choi I-G, Han D-P, Yun J, et al. Investigation of dominant non-radiative mechanisms as a function of current in InGaN/GaN light-emitting diodes. Appl Phys Exp 2013;6:052105.

[7] Kim K-S, Han D-P, Kim H-S, Shim J-I. Analysis of dominant carrier recombination mechanisms depending on injection current in InGaN green light emitting diodes. Appl Phys Lett 2014;104:091110.

[8] Masui H, Nakamura S, DenBaars SP. Technique to evaluate the diode ideality factor of light-emitting diodes. Appl Phys Lett 2010;96:073509.

[9] Malyutenko VK, Bolgov SS, Podoltsev AD. Current crowding effect on the ideality factor and efficiency droop in blue lateral InGaN/GaN light emitting diodes. Appl Phys Lett 2010;97:251110.

[10] Zhu D, Xu J, Noemaun AN, et al. The origin of the high diode-ideality factors in GaInN/GaN multiple quantum well light-emitting diodes. Appl Phys Lett 2009;94:081113.

[11] Lee GW, Shim J-I, Shin D-S. On the ideality factor of the radiative recombination current in semiconductor light-emitting diodes. Appl Phys Lett 2016;109:031104.

[12] Shim J-I, Shin D-S. Influences of the p-GaN growth temperature on the optoelectronic performances of GaN-based blue light-emitting diodes. IEEE J Quantum Electron 2016;52:3300208.

[13] Islam ABMH, Shim J-I, Shin D-S. Optoelectronic performance variations in InGaN/GaN multiple-quantum-well light-emitting diodes: effects of potential fluctuation. Materials 2018;11:743.

[14] Matioli E, Weisbunch C. Direct measurement of internal quantum efficiency in light emitting diodes under electrical injection. J Appl Phys 2000;87:3497.

[15] Getty A, Matioli E, Iza M. Electroluminescent measurement of the internal quantum efficiency of light emitting diodes. Appl Phys Lett 2009;94:181102.

[16] David A, Gardner NF. Droop in III-nitrides: comparison of bulk and injection contributions. Appl Phys Lett 2010;97:193508.

[17] Shin D-S, Han D-P, Oh J-I, Shim J-I. Study of droop phenomena in InGaN-based blue and green light-emitting diodes by temperature-dependent electroluminescence. Appl Phys Lett 2012;100:153506.

[18] Lin GB, Shan Q, Wang Y, et al. "U-turn" feature in the efficiency-versus-current curve of GaInN/GaN light-emitting diodes. Appl Phys Lett 2014;105:221116.

[19] Peter M, Laubsch A, Bergbauer W, et al. New developments in green LEDs. Phys Status Solidi A 2009;206:1125–9.

[20] Han D-P, Zheng D-G, Oh C-H, et al. Nonradiative recombination mechanisms in InGaN/GaN-based light-emitting diodes investigated by temperature-dependent measurements. Appl Phys Lett 2014;104:151108.

[21] Liu ML, Ye ZQ, Lei MS. Efficiency droop in blue InGaN/GaN single-quantum-well light-emitting diodes on the Si substrate. Semicond Sci Technol 2012;27:045010.

[22] Wang Y, Pan M, Li T. Comprehensive study of internal quantum efficiency of high-brightness GaN-based light-emitting diodes by temperature-dependent electroluminescence method. Proc SPIE 2014;9003:90030D.

[23] Titkov IE, Karpov YS, Yadav A, et al. Temperature-dependent internal quantum efficiency of blue high-brightness light-emitting diodes. IEEE J Quantum Electron 2014;50:911.

[24] Kawakami Y, Omae K, Kaneta A, et al. Radiative and nonradiative recombination processes in GaN-based semiconductors. Phys Status Solidi A 2001;41:183.

[25] Watanabe S, Yamada N, Nagashima M, et al. Internal quantum efficiency of highly-efficient $In_xGa_{1-x}N$-based near-ultraviolet light-emitting diodes. Appl Phys Lett 2003;83:4906.

[26] Honping Z, Guanguy L, Ronald AA, et al. Current injection efficiency induced efficiency-droop in InGaN quantum well light-emitting diodes. Solid-State Electron 2010;54:1119–24.

[27] Kivisaari P, Riuttanen L, Okasanen J, et al. Electrical measurement of internal quantum efficiency and extraction efficiency of III-N light-emitting diodes. Appl Phys Lett 2012;101:021113.

[28] Karpov S. ABC-model for interpretation of internal quantum efficiency and its droop in III-nitride LEDs: a review. Opt Quant Electron 2015;104:091110.

[29] Meneghini M, Trivellin N, Meneghesso G, et al. A combined electro-optical method for the determination of the recombination parameters in InGaN-based light-emitting diodes. J Appl Phys 2009;106:114508.

[30] Galler B, Drechsel P, Monnard R, et al. Influence of indium content and temperature on Auger-like recombination in InGaN quantum wells grown on (111) silicon substrates. Appl Phys Lett 2012;101:131111.

[31] Shatalov M, Chitnis A, Koudymov A, et al. Differential carrier lifetime in AlGaN based multiple quantum well deep UV light emitting diodes at 325 nm. Jpn J Appl Phys 2002;41:L1146.

[32] Nippert F, Karpov S, Pietzonka I, et al. Determination of recombination coefficients in InGaN quantum-well light-emitting diodes by small-signal time-resolved photoluminescence. Jpn J Appl Phys 2016;55:05FJ01.

[33] Nippert F, Karpov SY, Callsen G, et al. Temperature-dependent recombination coefficients in InGaN light-emitting diodes: hole localization, Auger processes, and the green gap. Appl Phys Lett 2016;109:161103.

[34] Schiavon D, Binder M, Peter M, et al. Wavelength-dependent determination of the recombination rate coefficients in single-quantum-well GaInN/GaN light emitting diodes. Phys Status Solidi B 2013;250:283–90.

[35] Verzellesi G, Saguatti D, Meneghini M, et al. Efficiency droop in InGaN/GaN blue light-emitting diodes: physical mechanisms and remedies. Appl Phys Lett 2013;114:071101.

[36] Piprek J. On the uncertainty of the Auger recombination coefficient extracted from InGaN/GaN light-emitting diode efficiency droop measurements. Appl Phys Lett 2016;106:101101.

[37] Weisbuch C, Piccardo M, Martinelli L, et al. The efficiency challenge of nitride light-emitting diodes for lighting. Phys Status Solidi A 2015;212:899–913.

[38] Dai Q, Shan Q, Wang J, et al. Carrier recombination mechanisms and efficiency droop in GaInN/GaN light-emitting diodes. Appl Phys Lett 2010;97:133507.

[39] Karpov SY. Effect of localized states on internal quantum efficiency of III-nitride LEDs. Phys Status Solidi RRL 2010;4:320–2.

[40] Galler B, Lugauer H-J, Binder M, et al. Experimental determination of the dominant type of Auger recombination in InGaN quantum wells. Appl Phys Express 2013;6:112101.

[41] Ryu H-Y, Kim H-S, Shim J-I. Rate equation analysis of efficiency droop in InGaN light-emitting diodes. Appl Phys Lett 2009;95:081114.

[42] Wang J, Wang L, Wang L, et al. An improved carrier rate model to evaluate internal quantum efficiency and analyze efficiency droop origin of InGaN based light-emitting diodes. J Appl Phys 2012;112:023107.

[43] Opdorp CV, Hooft GW. Method for determining effective nonradiative lifetime and leakage losses in double heterostructure lasers. J Appl Phys 1981;52:3827.

[44] Olshansky R, Su C, Manning J, et al. Measurement of radiative and nonradiative recombination rates in InGaAsP and AlGaAs light sources. IEEE J Quantum Electron 1984;20:8.

[45] Saito S, Zaima K, Tachibana K, et al. Estimation of internal quantum efficiency in InGaN-based light emitting diodes using electroluminescence decay times. Phys Status Solidi C 2008;5:2195–7.

[46] Altieri P, Jaeger A, Windisch R, et al. Internal quantum efficiency of high-brightness AlGaInP light-emitting devices. J Appl Phys 2005;98:086101.

[47] Yadav A, Titkova IE, Sokolovskii GS, et al. AlGaInP red-emitting light emitting diode under extremely high pulsed pumping. Proc SPIE 2016;9768:97681K.

[48] Meng X, Wang L, Hao Z, et al. Study on efficiency droop in InGaN/GaN light-emitting diodes based on differential carrier lifetime analysis. Appl Phys Lett 2016;108:013501.

[49] Han D-P, Oh C-H, Kim H, et al. Conduction mechanisms of leakage currents in InGaN/GaN-based light-emitting diodes. IEEE Trans Electron Devices 2015;62:2.

[50] Cao XA, Stokes EB, Sandvik PM, et al. Diffusion and tunneling currents in GaN/InGaN multiple quantum well light-emitting diodes. IEEE Electron Device Lett 2002;23:9.

[51] Shim J-I, Han D-P, Oh C-H, et al. Measuring the internal quantum efficiency of light-emitting diodes at an arbitrary temperature. IEEE J Quantum Electron 2018;54:2.

[52] Cao XA, LeBoeuf SF, Rowland LB, Yan CH, Liu H. Temperature-dependent emission intensity and energy shift in InGaN/GaN multiple-quantum-well light-emitting diodes. Appl Phys Lett 2003;82:3614.

[53] Chen D, Luo Y, Wang L, et al. Enhancement of electron-longitudinal optical phonon coupling in highly strained InGaN/GaN quantum well structures. J Appl Phys 2007;101:053712.

[54] Choi Y-H, Ryu G-H, Ryu H-Y. Evaluation of the temperature-dependent internal quantum efficiency and the light-extraction efficiency in a GaN-based blue light-emitting diode by using a rate equation model. J Korean Phys Soc 2016;69:1286.

[55] Titkov IE, Karpov SY, Yadav A, et al. Efficiency of true-green light emitting diodes: non-uniformity and temperature effects. Materials 2017;10:1323.

[56] Santhanam P, Gray DJ Jr, Ram RJ. Thermoelectrically pumped light-emitting diodes operating above unity efficiency. Phys Rev Lett 2012;108:097403.

[57] Gray DJ Jr, Santhanam P, Ram RJ. Design for enhanced thermos-electric pumping in light emitting diodes. Appl Phys Lett 2013;103:123503.

[58] Chen K, Xiao TP, Santhanam P, Yablonovitch E, Fan S. High-performance near-field electroluminescent refrigeration device consisting of a GaAs light emitting diode and a Si photovoltaic cell. J Appl Phys 2017;122:143104.